

# Salusin- $\beta$ participates in high glucose-induced HK-2 cell ferroptosis in a *Nrf-2*-dependent manner

WEN-JUAN WANG\*, XIA JIANG\*, CHANG-CHUN GAO and ZHI-WEI CHEN

Department of Nephrology, Center of Blood Purification,  
The Second People's Hospital of Nantong, Nantong, Jiangsu 226002, P.R. China

Received March 23, 2021; Accepted June 22, 2021

DOI: 10.3892/mmr.2021.12313

**Abstract.** Ferroptosis is critically involved in the pathophysiology of diabetic nephropathy (DN). As a bioactive peptide, salusin- $\beta$  is abundantly expressed in the kidneys. However, it is unclear whether salusin- $\beta$  participates in the pathologies of diabetic kidney damage by regulating ferroptosis. The present study found that high glucose (HG) treatment upregulated the protein expressions of salusin- $\beta$  in a dose- and time-dependent manner. Genetic knockdown of salusin- $\beta$  retarded, whereas overexpression of salusin- $\beta$  aggravated, HG-triggered iron overload, antioxidant capability reduction, massive reactive oxygen species production and lipid peroxidation in HK-2 cells. Mechanistically, salusin- $\beta$  inactivated nuclear factor erythroid-derived 2-like 2 (*Nrf-2*) signaling, thus contributing to HG-induced ferroptosis-related changes in HK-2 cells. Notably, the protein expression of salusin- $\beta$  was upregulated by ferroptosis activators, such as erastin, RSL3, FIN56 and buthionine sulfoximine. Pretreatment with ferrostatin-1 (a ferroptosis inhibitor) prevented the upregulated protein expression of salusin- $\beta$  in HK-2 cells exposed to HG. Taken together, these results suggested that a positive feedback loop between salusin- $\beta$  and ferroptosis primes renal tubular cells for injury in diabetes.

## Introduction

Diabetic nephropathy (DN) is one of the leading causes of mortality and morbidity in individuals with chronic kidney disease, accounting for 20-30% of deaths in patients with chronic kidney disease (1), and it is characterized by deposition

of extracellular matrix proteins, tubulointerstitial fibrosis, glomerular sclerosis, mesangial matrix and glomerular basement membrane expansion, as well as loss of waste removal functions over time (2,3). Currently, various factors are thought to be involved in the pathogenesis of DN, including hyperglycemia, oxidative stress, inflammatory response, activation of renin angiotensin system, lipid metabolism disorder, accumulation of advanced glycosylation end products, fibroblast activation, induction of transforming growth factor  $\beta$ -1 (*TGF- $\beta$ 1*) expressions, pyroptosis and depletion of adenosine triphosphate (4-7). Although our current understanding of the mechanisms of DN has substantially increased, the molecular mechanisms that lead to the occurrence and development of DN remain to be elucidated. Identification of novel therapeutic targets and strategies may uncover renoprotective effects in DN. Since the recognition of ferroptosis as an iron-dependent form of cell death in 2012 (8), interest in the functions of ferroptosis are continuously increasing (9). Ferroptosis occurs through two main types of pathway; transport dependent pathways and enzymatic regulatory pathways (10). Ferroptosis is dependent on intracellular iron and is primarily caused by a redox imbalance between oxidants and antioxidants in cells, resulting in the formation of free radicals and lipid oxidation products (10). Studies have demonstrated that ferroptosis is involved in the pathogenesis of inflammation, types of cancer, neurodegeneration and tissue injury (11,12). Emerging evidence has shown that ferroptosis is observed in several renal diseases, including nephrotoxic folic acid-induced acute kidney injury (13), rhabdomyolysis-induced renal damage (14), renal ischaemia-reperfusion injury (15), obesity-related kidney injury (16), carbon tetrachloride-induced renal toxicity (17) and DN (18,19). These findings suggest that modulation of ferroptosis may function as a future direction in the treatment of chronic or acute kidney injury.

With the aid of computer-assisted analysis of cDNA and genomic DNA sequence information, salusins are found to be translated from an alternatively spliced mRNA of torsion dystonia-related gene (*TOR2A*) (20). Proteolytic processing of prosalusin (216-amino acid) yields two related peptides of 28 and 20 amino acids, termed salusin- $\alpha$  and salusin- $\beta$ , respectively (20). Salusins are widely expressed in human, rat and mouse tissues, such as the central nervous system, digestive system, vasculature and kidneys (20-22). It is noteworthy to mention that salusin- $\alpha$  and salusin- $\beta$  serve critical

---

*Correspondence to:* Dr Zhi-Wei Chen, Department of Nephrology, Center of Blood Purification, The Second People's Hospital of Nantong, 43 Xinglong Road, Tangzha, Nantong, Jiangsu 226002, P.R. China  
E-mail: jinmeicnt99@sohu.com

\*Contributed equally.

**Key words:** diabetic nephropathy, ferroptosis, salusin, nuclear factor erythroid-derived 2-like 2, reactive oxygen species

roles in the pathogenesis of cardiovascular and metabolic diseases (23-25). Recently, it was found that renal salusin- $\alpha$  levels are lower in diabetic rats and exogenous salusin- $\alpha$  markedly ameliorates the development of DN (26). Evidence is emerging that salusin- $\beta$  may serve a role in the etiologies of diabetic kidney disease. For example, circulating levels of salusin- $\beta$  tend to be higher in diabetic patients (27-29). Patients undergoing hemodialysis who exhibit higher serum levels of salusin- $\beta$  and higher salusin- $\beta$  levels may have cardiovascular risk implications (30). Immunohistochemical analysis has demonstrated that salusin- $\beta$  is mainly expressed in epithelium cells of the glomeruli and proximal and distal tubule cells (31). The expression of salusin- $\beta$  is increased in kidneys from rats with insulin resistance (31). These studies hint a possible role of salusin- $\beta$  in diabetes-induced renal damage. Notably, salusin- $\beta$  is a potential pro-oxidant in cardiomyocytes (32), vascular smooth muscle cells (33), endothelial cells (34) and kidney cells (35). These studies suggest that salusin- $\beta$  may be a critical regulator in oxidative stress-related diseases. In addition, the cellular redox system governs a pervasive non-apoptotic form of cell death, ferroptosis (36). These results prompted the investigation of the roles of salusin- $\beta$  in diabetes-related kidney damage and the involved downstream signaling pathways, such as ferroptosis-related events, are also probed.

## Materials and methods

**Chemicals and reagents.** DMEM/F-12 medium (cat. no. 12400-024), fetal bovine serum (FBS; cat. no. 16140-071), penicillin and streptomycin antibiotic mixture (cat. no. 15140122) and cell culture supplies were obtained from Gibco (Thermo Fisher Scientific, Inc.). D-glucose (cat. no. G8270), D-mannitol (cat. no. M4125), 2',7'-dichlorofluorescein diacetate (DCFH-DA; cat. no. D6883), 4',6'-diamidino-2-phenylindole dihydrochloride (DAPI; cat. no. D8417), ferrostatin-1 (cat. no. SML0583), bardoxolone methyl (CDDO Methyl Ester; cat. no. SMB00376), erastin (cat. no. E7781) and buthionine sulfoximine (cat. no. B2515) were purchased from Sigma-Aldrich; Merck KGaA. RSL3 (cat. no. S8155) and FIN56 (cat. no. S8254) were obtained from Selleck Chemicals. Antibody against salusin- $\beta$  (cat. no. PAC026Hu01) and enzyme linked immunosorbent assay (ELISA) kits for salusin- $\beta$  (cat. no. CEC026Hu) measurement were obtained Wuhan USCN Business Co., Ltd. Click-iT Plus EdU (5-ethynyl-2'-deoxyuridine) Alexa Fluor 594 imaging kits were procured from Thermo Fisher Scientific, Inc. (cat. no. C10639). Goat Anti-Rabbit IgG H&L (Alexa Fluor 488; cat. no. ab150077) was purchased from Abcam. The specific primers used in the present study were synthesized by Santa Cruz Biotechnology, Inc. Control short interfering (si)RNA (cat. no. sc-44239) and nuclear factor-erythroid-2-related factor 2 (*Nrf-2*) siRNA cat. no. (sc-37030) were bought from Santa Cruz Biotechnology, Inc. Lentivirus particles carrying salusin- $\beta$  short hairpin (sh)RNA or negative control shRNA were produced by Jiman Biotechnology (Shanghai) Co., Ltd., as previously described (35,37). Lentivirus empty vectors or vectors expressing salusin- $\beta$  were constructed by Jiman Biotechnology (Shanghai) Co., Ltd as previously described (33,35,38). Antibodies against  $\beta$ -actin (cat. no. 66009-1-Ig or cat. no. 20536-1-AP) and

HRP-conjugated secondary antibodies (cat. nos. SA00001-1 and SA00001-2) were obtained from ProteinTech Group, Inc. Antibodies against glutathione peroxidase 4 (*GPX4*; cat. no. 52455), solute carrier family 7 (cationic amino acid transporter, y+ system) member 11 (*SLC7A11*; cat. no. 12691), ferritin heavy polypeptide 1 (*FTH-1*; cat. no. 4393), transferrin receptor 1 (*TFR-1*; cat. no. 13113) and *Nrf-2* (cat. no. 12721) were purchased from Cell Signaling Technology, Inc. Cell Counting Kit-8 (CCK-8; cat. no. G021-1-1), lactate dehydrogenase (LDH) release kits (cat. no. A020-2-2), malondialdehyde (MDA) assay kit (cat. no. A003-1-2) and reduced glutathione (GSH) assay kits (cat. no. A006-2-1) were purchased from Nanjing Jiancheng Bioengineering Institute. An iron assay kit (cat. no. ab83366) was from Abcam. The selected concentrations of chemicals were in accord with previously published papers (19,39,40).

**Cell culture.** Human proximal tubular (HK-2) cells were procured from the American Type Culture Collection (cat. no. CRL-2190). HK-2 cells were cultured in DMEM/F-12 medium contained 10% FBS, streptomycin (100 mg/ml) and penicillin (100 U/ml) under a humidified atmosphere of 5% CO<sub>2</sub> at 37°C. When HK-2 cells reached ~70-80% confluence, these cells were challenged by 30 mM glucose (Sigma-Aldrich; Merck KGaA) at different time points. D-mannitol was used as a hyperosmolar control in the current study (5.5 mM D-glucose plus 24.5 mM D-mannitol) (41). In some experiments, HK-2 cells were pretreated with bardoxolone methyl (100 nM), or Ferrostatin-1 (1  $\mu$ M) for 30 min before high glucose (HG) stimulation.

**Western blotting.** After treatment, HK-2 cells were washed with ice-cold PBS and lysed in RIPA lysis buffer (20 mM Tris at pH 7.5, 150 mM NaCl, 1 mM EDTA and 2% Triton X-100) supplemented with protease inhibitor cocktail (Roche Diagnostics) and the protein contents were determined by using BCA colorimetric protein kit (P0012; Beyotime Institute of Biotechnology). The sodium dodecyl sulfate-polyacrylamide gel electrophoresis loading buffer was added into cell lysates and boiled for 5 min. Samples and pre-stained markers were added as required. Equal amount of cell lysates (30  $\mu$ g) was separated onto SDS-PAGE gels (8-12%) and transferred onto polyvinylidene fluoride membranes. Membranes were sealed with 5% skimmed milk powder for 1 h at room temperature, followed by incubation with primary antibodies at 4°C overnight. The following primary antibodies were used: Salusin- $\beta$  (1:500; cat. no. PAC026Hu01; Wuhan USCN Business Co., Ltd),  $\beta$ -actin (1:1,000; cat. no. 66009-1-Ig; ProteinTech Group, Inc.), *GPX4* (1:1,000; cat. no. 52455; Cell Signaling Technology, Inc.), *SLC7A11* (1:1,000; cat. no. 12691; Cell Signaling Technology, Inc.), *FTH-1* (1:1,000; cat. no. 4393; Cell Signaling Technology, Inc.), *TFR-1* (1:1,000; cat. no. 13113; Cell Signaling Technology, Inc.) and *Nrf-2* (1:1,000; cat. no. 12721; Cell Signaling Technology, Inc.). Membranes were then incubated with horseradish peroxidase-conjugated secondary antibodies (1:5,000; cat. nos. SA00001-1 and SA00001-2; ProteinTech Group, Inc.) for 1 h at room temperature. Immunodetection was conducted using an ECL system (Fusion FX7 imaging system; Vilber China). Protein

expression was semi-quantified using Image Lab software (version 5.2.1; Bio-Rad Laboratories, Inc.).

**Immunofluorescence staining.** HK-2 cells were fixed with 4% paraformaldehyde for 20 min at room temperature. The fixed cells were then permeabilized with 0.1% Triton X-100 for 10 min at room temperature and 5% goat serum (cat. no. C0265; Beyotime Institute of Biotechnology) for 1 h. The expressions of salusin- $\beta$  in HK-2 cells were detected by incubation of primary antibody against salusin- $\beta$  at 4°C overnight. Afterwards, these cells were incubated with Goat Anti-Rabbit IgG H&L (Alexa Fluor 488) for 1 h at 37°C and the nucleus was stained by DAPI for 10 min at room temperature. The positive immunofluorescence images were captured by a fluorescence microscopy (Olympus BX6 with DP72 camera; Olympus Corporation; magnification, x200). A total of six visual fields in each group were randomly selected in each group.

**Reverse transcription-quantitative (RT-q) PCR.** Total RNA was isolated from cells ( $2 \times 10^5$ ) by TRIzol® reagent (cat. no. 9108; Thermo Fisher Scientific, Inc.). All steps were performed according to the manufacturer's protocols. The purity and concentration of RNA were detected using NanoDrop (Thermo Fisher Scientific, Inc.). The first cDNA synthesis was conducted using GoScript Reverse Transcription System (Promega Corporation) in the presence of 0.5 g of total RNA in each sample. Following the manufacturer's instructions, RT-qPCR was carried out using the qPCR SYBR-Green Master Mix (cat. no. 11119ES60; Shanghai Yeasen Biotechnology Co., Ltd.) under the Applied Biosystems 7500 Real Time PCR System (Applied Biosystems; Thermo Fisher Scientific, Inc.). The following thermocycling conditions were used for qPCR: Initial denaturation at 95°C for 120 sec, followed by 40 amplification cycles at 95°C for 15 sec, and annealing and extension at 60°C for 20 sec. The relative expression levels were calculated based on the  $2^{-\Delta\Delta C_t}$  method (42). These experiments were repeated three independent times. The primer sequences used for RT-qPCR are listed in Table S1.

**Enzyme-linked immunosorbent assay (ELISA).** The levels of salusin- $\beta$  in cellular lysate were analyzed through the commercial ELISA kits according to the instructions as previously described (43,44). Briefly, the samples and diluted standards (50  $\mu$ l) were added into the appropriate wells, respectively. 50  $\mu$ l of Detection Reagent A was added into each well and incubated for 1 h at 37°C. After washing three times with 1X Wash Solution, 100  $\mu$ l of Detection Reagent B working solution was added into each well and incubated for 30 min at 37°C. Substrate Solution and Stop Solution were subsequently added into each well and the liquid turned yellow. The measurement of optical density was performed using a microplate reader (SYNERGY H4; BioTek Instruments, Inc.) at 450 nm immediately. The levels of salusin- $\beta$  were expressed as pg per mg protein by normalizing to the protein contents in each sample.

**Determination of cell viability.** Cell viability was evaluated using the CCK-8 according to the manufacturer's instructions. In brief, HK-2 cells were seeded onto 96-well plates

( $1 \times 10^4$  cells/well) and treated with normal glucose (NG) and high glucose (HG), respectively. The culture medium was replaced with 100  $\mu$ l fresh medium supplemented with 10  $\mu$ l of the CCK-8 solution in each well. After incubating for 2 h at 37°C, measurement of the absorbance at 450 nm was carried out by using a microplate reader (SYNERGY H4; BioTek Instruments, Inc.). In addition, Click-iT Plus EdU (5-ethynyl-2'-deoxyuridine) Alexa Fluor™ 594 imaging kits were used for measurement of HK-2 cell proliferation according to the manufacturer's protocols. The red and blue fluorescence signals were imaged by a fluorescence microscopy (Olympus BX6 with DP72 camera; Olympus Corporation; magnification, x200). A total of 6 visual fields were randomly selected in each group and the average number of positive cells was calculated.

**Cell transfection.** HK-2 cells in logarithmic growth were transduced with lentivirus particles carrying salusin- $\beta$  shRNA or negative control shRNA ( $10^9$  titer/ml; MOI=50, 50  $\mu$ l lentivirus particles per  $1 \times 10^6$  cells) for 48 h at 37°C and then challenged by HG stimulation for another 48 h at 37°C. For overexpression of salusin- $\beta$  in HK-2 cells, HK-2 cells were transduced with lentivirus expressing salusin- $\beta$  vectors or empty vectors ( $10^{10}$  titer/ml; MOI=50, 50  $\mu$ l lentivirus particles per  $1 \times 10^6$  cells) for 48 h at 37°C before administration of NG or HG for 48 h. After that, cells were harvested for biochemical testing at the desired time points. For *Nrf-2* knockdown, HK-2 cells were plated the day before siRNA transfection. A non-targeting control siRNA (50 nM) and *Nrf-2* siRNA (50 nM) were transduced to HK-2 cells for 48 h at 37°C by using Lipofectamine® 2000 (Invitrogen; Thermo Fisher Scientific, Inc.) following the manufacturer's instructions. The medium was changed after 4–6 h of transfection. Subsequent experiments were performed at 48 h post-transfection.

**Iron assay.** Total iron levels in cell lysates were quantified by an iron assay kit (ab83366, Abcam). Briefly, the collected HK-2 cells were lysed in the iron assay buffer and the supernatants were obtained by centrifugation at 16,000 x g for 10 min at 4°C. A total of 5 ml of iron reducing agent was mixed into cell samples (50 ml) for total iron analysis. Next, the iron probe solution (100 ml) was added and incubated for 1 h at 25°C under dark conditions. Later, the absorbance at the wavelength of 593 nm was detected by spectrophotometry.

**Measurement of MDA contents.** The collected cells were homogenized by the MDA lysis buffer and the supernatants were collected after centrifugation at 13,800 x g for 10 min at 4°C. The MDA concentrations in cell lysates were assessed using a lipid peroxidation assay kit according to the manufacturer's instructions. In short, 200  $\mu$ l of the supernatant from each homogenized sample was placed into a tube, followed by incubation of the thiobarbituric acid solution (200  $\mu$ l) for 40 min at 95°C. These samples were cooled to room temperature and centrifuged (1,500 x g for 10 min) to remove insoluble sediment. The supernatants were collected and the absorbance was measured at 532 nm using a microplate reader (SYNERGY H4; BioTek Instruments, Inc.).

**Measurement of GSH levels.** HK-2 cells were washed with ice-cold PBS and homogenized by vibrating homogenizer



with cold PBS and the supernatants were collected after centrifugation at 13,800  $\times$  g for 10 min at 4°C. GSH assay mixture (125  $\mu$ l) was added into each well for 5 min at room temperature and the optical density was determined at the wavelength of 405 nm. The concentrations of GSH were then quantified by comparing the optical density of the samples to the standard curve, respectively.

**Measurement of reactive oxygen species (ROS).** Intracellular ROS levels in HK-2 cells were evaluated by dichloro-dihydro-fluorescein diacetate (DCFH-DA) staining as previously described (45,46). HK-2 cells were initially cultured in 6-well plates for 48 h and DCFH-DA fluorescent dye (10  $\mu$ M) was added and incubated for 20 min at 37°C in the dark and then were washed with PBS. The fluorescence intensity was measured by a fluorescence microscope (Olympus BX6 with DP72 camera; Olympus Corporation) with an excitation wavelength at 488 nm and an emission wavelength at 525 nm. The images were observed and captured in 10 randomly selected fields of view from 4-6 repeated experiments in 1-2 randomly selected fields of view (magnification,  $\times$ 200).

**LDH release assay.** LDH contents were measured using LDH cytotoxicity assay kits as previously reported (47). The standards and culture supernatants were obtained and added into the appropriate wells (20  $\mu$ l), matrix buffer (25  $\mu$ l) and coenzyme I (5  $\mu$ l) were sequentially added. The liquid system was incubated for 15 min at 37°C. Later, 2,4-Dinitrophenylhydrazine (25  $\mu$ l) was added and incubated for 15 min at 37°C. Sodium hydroxide solution (0.4 M, 250  $\mu$ l) were then added and incubated for 5 min at room temperature. The reactions were read at 450 nm by using a microtiter plate reader (SYNERGY H4; BioTek Instruments, Inc.). Mean LDH release of control cells was indexed to 100%, the value used for normalization.

**Statistical analysis.** Results were expressed as mean  $\pm$  standard deviation. All results were analyzed by GraphPad Prism 6.0 (GraphPad Software, Inc.). All data were tested for normality and equal variance. If the data passed these tests, comparisons between two groups were made by unpaired Student's *t* tests. One way ANOVA was used for multiple-group comparisons. When ANOVA was significant, post hoc testing of differences between groups was conducted by using Bonferroni tests. The independent experiments were repeated at least four times.  $P < 0.05$  was considered to indicate a statistically significant difference.

## Results

**Expression of salusin- $\beta$  in HG-incubated HK-2 cells.** To test whether HG altered salusin- $\beta$  expression in HK-2 cells, HK-2 cells were treated with increasing doses of glucose at various time points. Upon HG treatment (25 mM), the protein expression of salusin- $\beta$  was upregulated in HK-2 cells and this was further increased with increasing glucose concentrations, reaching its maximal effect at 30 mM (Fig. 1A and B). Thus, the dose of glucose was selected as 30 mM for the following experiments. Time-course experiments showed that the protein expression of salusin- $\beta$  was increased slightly after HG treatment for 24 h

(Fig. 1C and D). However, the protein expression of salusin- $\beta$  was markedly augmented in HK-2 cells exposed to HG for 48 and 72 h (Fig. 1C and D). Accordingly, HG treatment for 48 h was chosen as a model of cell damage during the subsequent experiments. Furthermore, HG-induced upregulation of salusin- $\beta$  in HK-2 cells was confirmed by immunofluorescence (Fig. 1E), RT-qPCR (Fig. 1F) and ELISA results (Fig. 1G), respectively. To study the effects of osmolality on the expression of salusin- $\beta$ , D-mannitol was used as a hyperosmolar control (5.5 mM D-glucose plus 24.5 mM D-mannitol) (41,48). Notably, the protein and mRNA expressions of salusin- $\beta$  were markedly incremented in HG-incubated HK-2 cells, but not in hyperosmolar D-mannitol-treated cells (Fig. S1A-C). These results suggested that aberrant expressions of salusin- $\beta$  in HK-2 cells were an effect of glucotoxicity, rather than from hyperglycemia-induced hyperosmolality.

**Effects of salusin- $\beta$  knockdown on HG-induced ferroptosis in HK-2 cells.** Previous studies have highlighted the importance of ferroptosis in the development of DN as inhibition of ferroptosis can effectively delay the progression of DN (18,19). It is reported that salusin- $\beta$  serves as an inducer of oxidative stress in HK-2 cells through increased ROS levels and decreased GSH activities (35), key characteristics of ferroptosis (15,49). On this basis it was hypothesized that salusin- $\beta$  might be involved in HG-induced ferroptosis in HK-2 cells. To test this hypothesis, the protein and mRNA expressions of ferroptosis-related genes, such as *GPX4*, *SLC7A11*, *FTH-1* and *TFR-1*, in salusin- $\beta$ -deficient HK-2 cells under HG conditions were examined. Similar to a previous report (19), the protein expressions of *GPX4*, *SLC7A11* and *FTH-1* were downregulated, while *TFR-1* protein expression was upregulated in HK-2 cells exposed to HG (Fig. 2A and B). However, deletion of salusin- $\beta$  (Fig. S2A) reversed abnormal expressions of these proteins induced by HG (Fig. 2A and B). In line with this, RT-qPCR results showed a parallel change in mRNA expression levels of *GPX4*, *SLC7A11*, *FTH-1* and *TFR-1* (Fig. 2C). Meanwhile, incubation of HK-2 cells with HG promoted the concentration of iron and induced the end products of lipid peroxidation, MDA, accompanied by a decrease in GSH contents (Fig. 2D-F). Notably, the ferroptosis-related changes in HG-induced HK-2 cells were rescued when salusin- $\beta$  was absent (Fig. 2D-F). In addition, knockdown of salusin- $\beta$  attenuated HG-elicited massive generation of ROS, as evidenced by DCFH-DA staining (Fig. 2G and H). Importantly, knockdown of salusin- $\beta$  significantly inhibited HG-triggered cell viability decline and LDH release, suggesting the protective effects of salusin- $\beta$  deficiency against HG-induced cytotoxicity in HK-2 cells (Fig. 2I-K). Furthermore, induction of ferroptosis and decreased cell viability were not observed in D-mannitol-incubated HK-2 cells (Fig. S1D-G). These preliminary results suggested that the antagonistic effects of salusin- $\beta$  knockdown on ferroptosis may be dependent on the expressions of antioxidant genes (*GPX4* and *SLC7A11*) and iron metabolism-related genes (*FTH-1* and *TFR-1*).

**Effects of salusin- $\beta$  overexpression on HG-induced ferroptosis in HK-2 cells.** In contrast to the above results, overexpression of salusin- $\beta$  (Fig. S2B) aggravated the effects of HG on the



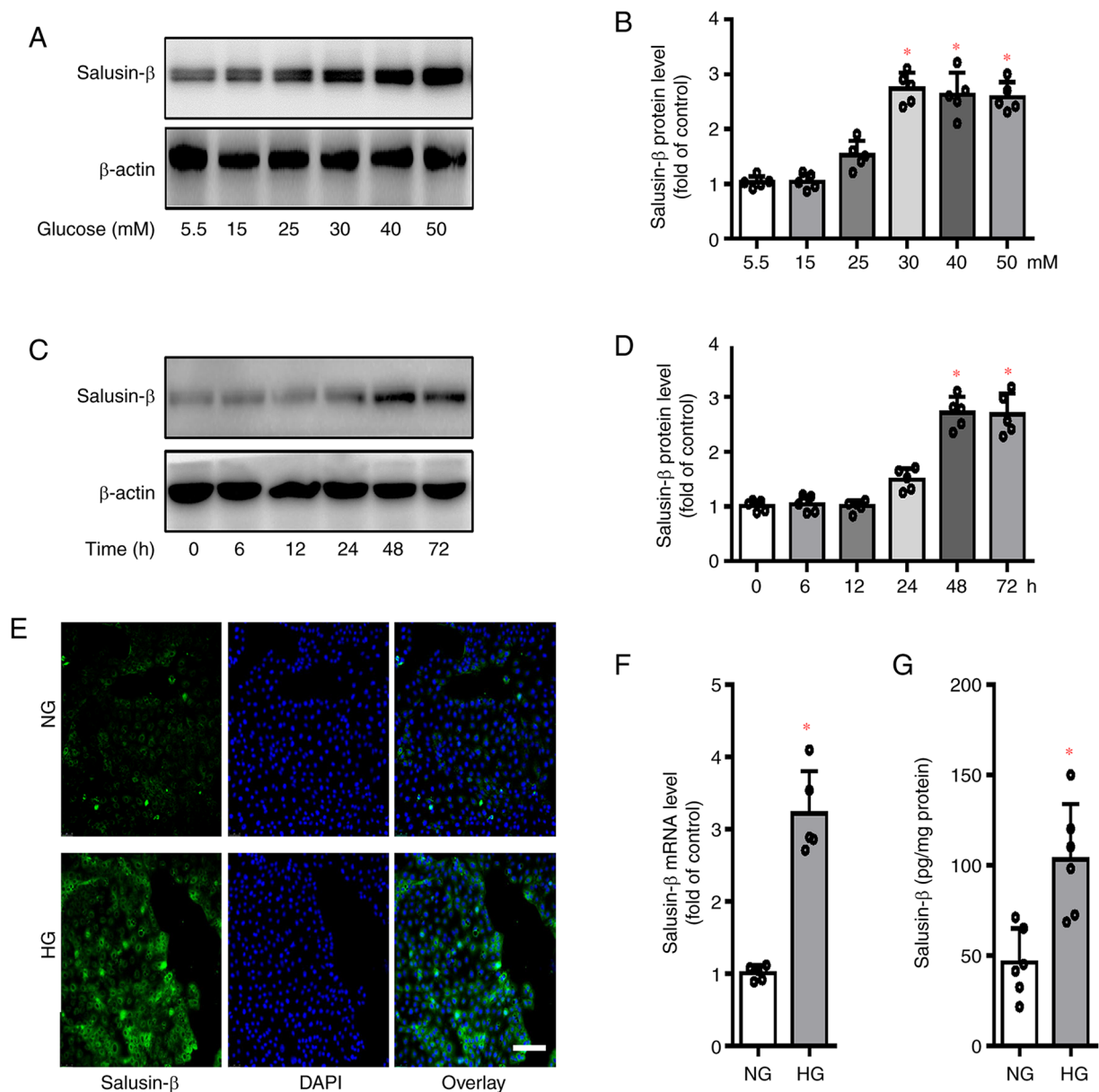


Figure 1. Expression of salusin- $\beta$  in HG-incubated HK-2 cells. (A and B) HK-2 cells were incubated with various doses of glucose (5.5, 15, 25, 30, 40 and 50 mM) for 48 h, and the protein expression of salusin- $\beta$  examined. (C and D) HK-2 cells were incubated with high glucose (HG, 30 mM) for various time points and the protein expression of salusin- $\beta$  was examined. (E) Effects of HG (30 mM) incubation for 48 h on the protein expression of salusin- $\beta$  as determined by immunofluorescence staining. Scale bar=200  $\mu$ m. (F) Effects of HG (30 mM) incubation for 48 h on the mRNA expression of salusin- $\beta$  determined by reverse transcription-quantitative PCR. (G) Effects of HG (30 mM) incubation for 48 h on the protein expression of salusin- $\beta$  as determined by ELISA. Data are presented as the mean  $\pm$  SD (n=4-5 per group). \*P<0.05 vs. 5.5 mM, 0 h, or NG. n=4-5 for each group. HG, high glucose; NG, normal glucose.

protein (Fig. 3A-B) and mRNA (Fig. 3C) expressions of *GPX4*, *SLC7A11*, *FTH-1* and *TFR-1* in HK-2 cells. Notably, salusin- $\beta$  overexpression itself also changed the expressions of *GPX4*, *SLC7A11*, *FTH-1* and *TFR-1* in HK-2 cells at both protein and mRNA levels (Fig. 3A-C), indicating the critical implication of salusin- $\beta$  in the process of ferroptosis. In addition, ectopic overexpression of salusin- $\beta$  further deteriorated HG-induced ferroptosis in HK-2 cells, as manifested by more iron accumulation, MDA contents and lower GSH contents (Fig. 3D-F). DCFH-DA staining results showed that overexpression of salusin- $\beta$  worsened the effects of HG on ROS generation in HK-2 cells (Fig. 3G and H). HG-induced decrease in cell viability and increase in LDH release were further exacerbated by ectopic overexpression of salusin- $\beta$

(Fig. 3I and K). Additionally, salusin- $\beta$  overexpression led to spontaneous cytotoxicity on HK-2 cells, as indicated by measurement of cell viability and LDH release (Fig. 3I and K).

**Effects of salusin- $\beta$  on *Nrf-2* signaling in HG-induced HK-2 cells.** As a master antioxidant regulatory transcription factor, *Nrf-2* is found to prevent ferroptosis-related cell death via upregulating antioxidant enzymes, including heme oxygenase-1 (*HO-1*), *GPX4* and *SLC7A11* (50). In addition, *Nrf-2* serves a vital role in the regulation of ferroptosis-related genes, such as genes for thiol-dependent antioxidant system, ion metabolism, enzymatic detoxification of reactive carbonyl species and carbonyls, nicotinamide adenine dinucleotide phosphate system and ROS generation from mitochondria

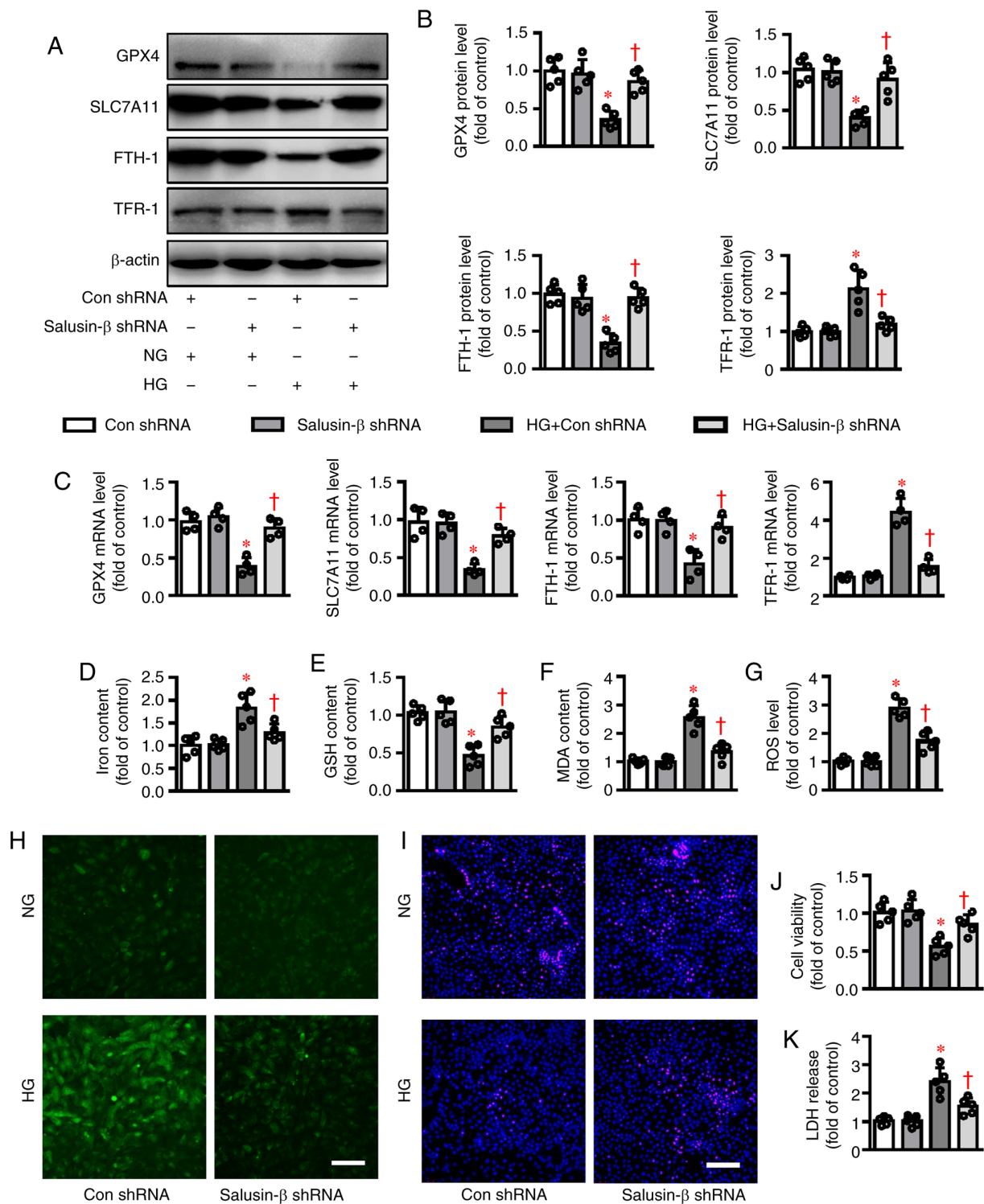


Figure 2. Effects of salusin- $\beta$  knockdown on HG-induced ferroptosis in HK-2 cells. HK-2 cells in logarithmic growth were transduced with lentivirus particles carrying salusin- $\beta$  shRNA or negative control shRNA at MOI=50 for 48 h and then challenged by HG stimulation for another 48 h. (A) Representative blot images and (B) quantitative analysis of *GPX4*, *SLC7A11*, *FTH-1* and *TFR-1*. (C) Relative mRNA levels of *GPX4*, *SLC7A11*, *FTH-1* and *TFR-1*. (D) Iron contents. (E) GSH contents. (F) MDA levels. (G and H) ROS generation was assessed by dichloro-dihydro-fluorescein diacetate fluorescence. (I) The proliferation of HK-2 cells was evaluated by EdU staining. (J) The cell proliferation was assessed by CCK-8 assay. (K) The cytotoxicity was determined by LDH release assay. Scale bar=200  $\mu$ m. Data are presented as the mean  $\pm$  SD (n=4-5 per group). \* $P < 0.05$  vs. Con shRNA. † $P < 0.05$  vs. HG + Con shRNA. HG, high glucose; NG, normal glucose; sh, short hairpin RNA; MOI, multiplicity of infection; *GPX4*, glutathione peroxidase 4; *SLC7A11*, solute carrier family 7 (cationic amino acid transporter, y+ system) member 11; *FTH-1*, ferritin heavy polypeptide 1; *TFR-1*, transferrin receptor 1; GSH, glutathione; MDA, malondialdehyde; ROS, reactive oxygen species; LDH, lactate dehydrogenase; Con, control.

or extra-mitochondria (51). Activation of *Nrf-2* signaling is anticipated to open up a novel way to treat ferroptosis-associated diseases, including DN (19). As expected, Bardoxolone

methyl, an inducer of *Nrf-2* (Fig. 4A and B), upregulated the mRNA expression levels of *GPX4* and *SLC7A11* and reversed HG-induced inhibition of *GPX4* and *SLC7A11* mRNA levels

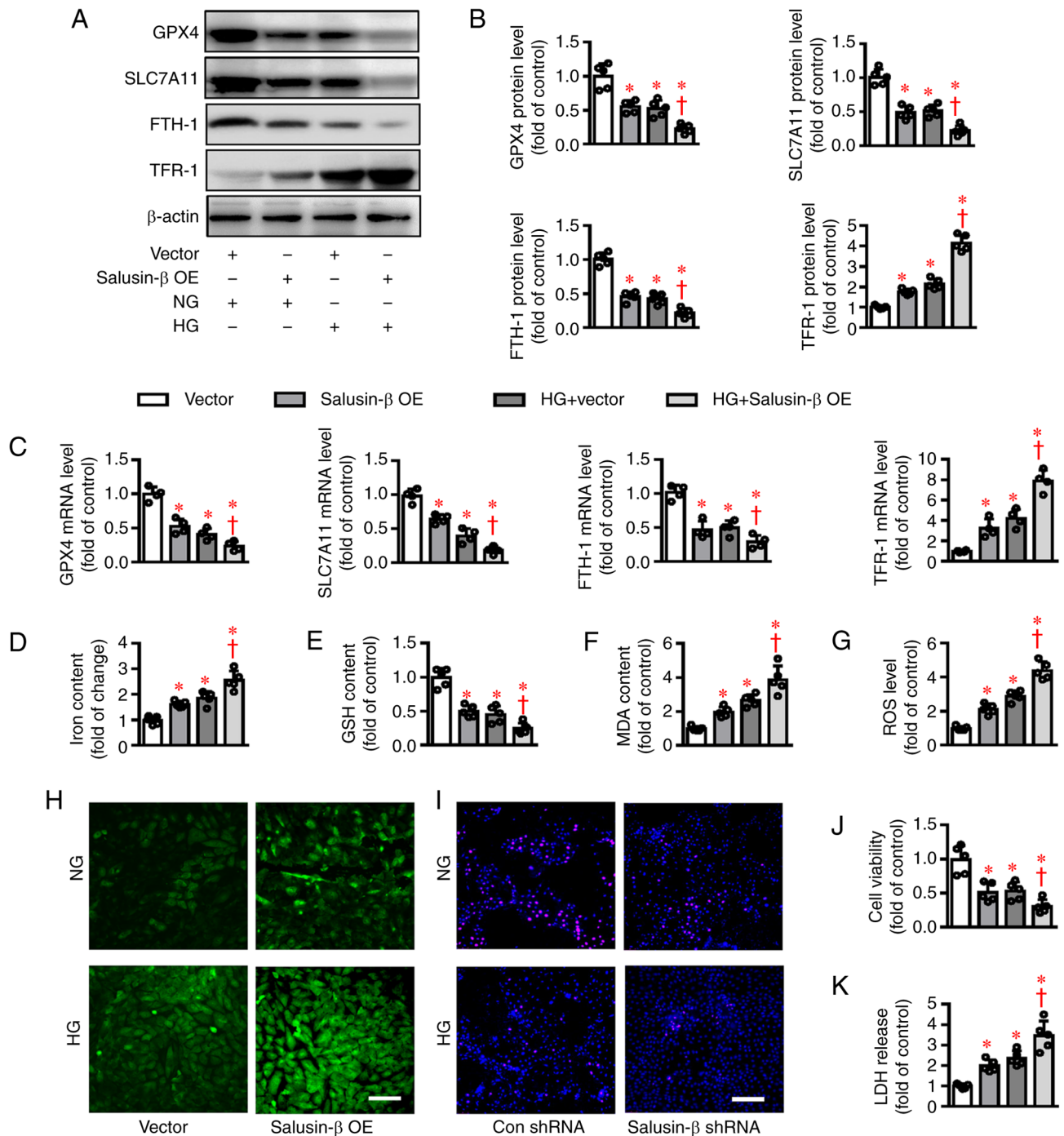


Figure 3. Effects of salusin- $\beta$  overexpression on HG-induced ferroptosis in HK-2 cells. HK-2 cells were transduced with lentivirus expressing salusin- $\beta$  vectors or empty vectors (MOI=50) for 48 h before administration of NG or HG for another 48 h. (A) Representative blot images and (B) quantitative analysis of *GPX4*, *SLC7A11*, *FTH-1* and *TFR-1*. (C) Relative mRNA levels of *GPX4*, *SLC7A11*, *FTH-1* and *TFR-1*. (D) Iron contents. (E) GSH contents. (F) MDA levels. (G and H) ROS generation was assessed by dichloro-dihydro-fluorescein diacetate fluorescence. (I) The proliferation of HK-2 cells was evaluated by EdU staining. (J) The cell proliferation was assessed by CCK-8 assay. (K) The cytotoxicity was determined by LDH release assay. Scale bar=200  $\mu$ m. Data are presented as the mean  $\pm$  SD (n=4-5 per group). \*P<0.05 vs Vector.  $\dagger$ P<0.05 vs. HG + Vector. HG, high glucose; MOI, multiplicity of infection; NG, normal glucose; sh, short hairpin RNA; *GPX4*, glutathione peroxidase 4; *SLC7A11*, solute carrier family 7 (cationic amino acid transporter, y+ system) member 11; *FTH-1*, ferritin heavy polypeptide 1; *TFR-1*, transferrin receptor 1; GSH, glutathione; MDA, malondialdehyde; ROS, reactive oxygen species; LDH, lactate dehydrogenase; Con, control; OE, overexpression.

(Fig. 4C and D). The contents of iron and MDA were enhanced (Fig. 4E and G), whereas GSH levels and cell viability were diminished in HK-2 cells challenged by HG (Fig. 4F and 4H) and these effects were noticeably dampened by application of Bardoxolone methyl. The present study next investigated whether *Nrf-2* signaling was involved in salusin- $\beta$ -mediated

ferroptosis in HG-stimulated HK-2 cells. As shown in Fig. 4I, the protein expression of *Nrf-2* was significantly increased in HG-incubated cells being treated with salusin- $\beta$  shRNA compared with the control shRNA group. By contrast, the decreased expression of *Nrf-2* was further exacerbated by overexpression of salusin- $\beta$  in HG-stimulated HK-2 cells



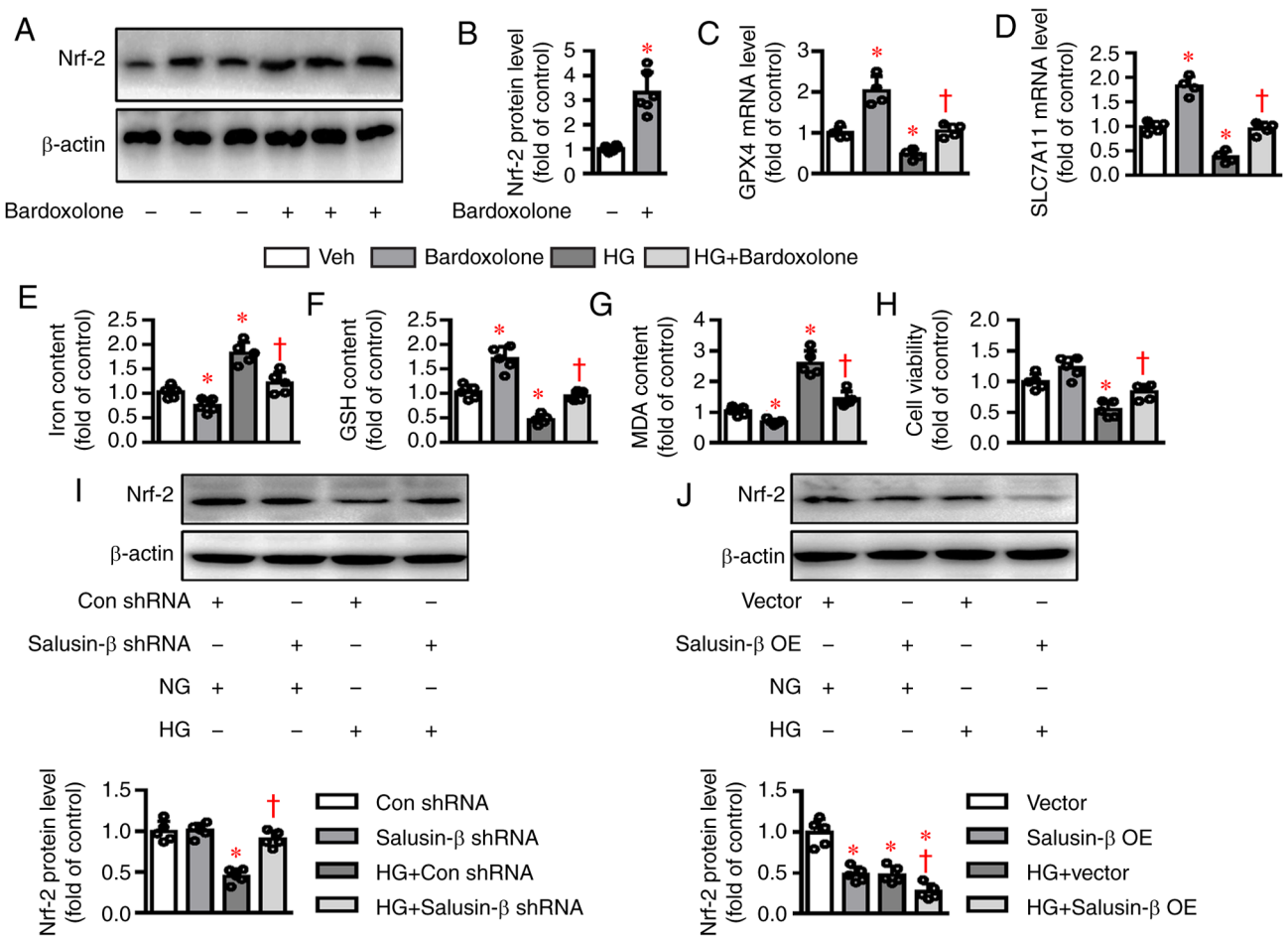


Figure 4. Effects of salusin- $\beta$  on *Nrf-2* signaling in HG-induced HK-2 cells. (A and B) Effects of Bardoxolone methyl (100 nM) incubation for 24 h on the protein expression of *Nrf-2*. (C and D) HK-2 cells were pretreated with *Nrf-2* inducer bardoxolone methyl (100 nM) for 30 min and then challenged by HG (30 mM) for 48 h. mRNA levels of *GPX4* and *SLC7A11* were examined by reverse transcription-quantitative PCR. (E) Effects of bardoxolone methyl (100 nM) on (E) iron contents (F) GSH contents and (G) MDA contents induced by HG. (H) Effects of bardoxolone methyl (100 nM) on cell viability decline induced by HG. (I) Silencing of salusin- $\beta$  restored the protein expression of *Nrf-2* in HG-incubated HK-2 cells. (J) Overexpression of salusin- $\beta$  further inhibited the protein expression of *Nrf-2* in HG-incubated HK-2 cells. Data are presented as the mean  $\pm$  SD ( $n=4-5$  per group). \* $P<0.05$  vs. Veh, Con shRNA, or Vector. † $P<0.05$  vs. HG, HG + Con shRNA, or HG + Vector. *Nrf-2*, nuclear factor erythroid-derived 2-like 2; *GPX4*, glutathione peroxidase 4; *SLC7A11*, solute carrier family 7 (cationic amino acid transporter, y+ system) member 11; Veh, Vehicle; Con, Control; sh, short hairpin RNA; NG, normal glucose; HG, high glucose; OE, overexpression.

(Fig. 4J). The data clearly demonstrated that salusin- $\beta$  might be responsible for HG-induced ferroptosis via inhibiting the *Nrf-2* signaling pathway.

To further verify the implication of the *Nrf-2* signaling cascade in salusin- $\beta$ -mediated ferroptosis in HK-2 cells, *Nrf-2* siRNA and *Nrf-2* inducer Bardoxolone methyl were used in the present study. In the absence of *Nrf-2* (Fig. S3), the suppressive effects of salusin- $\beta$  shRNA on HG-induced cell damage, including iron deposition, GSH deletion, MDA accumulation and cell viability decline, were abolished (Fig. 5A and D). In parallel to this, the stimulatory effects of salusin- $\beta$  on HG-induced ferroptosis occurrence were clearly compromised by Bardoxolone methyl pretreatment (Fig. 5E-H). Collectively, the molecular mechanism by which salusin- $\beta$  contributed to ferroptosis appeared to involve *Nrf-2*-mediated regulation of antioxidant system and ion metabolism.

**Expression of salusin- $\beta$  during the process of ferroptosis.** The above results demonstrated that salusin- $\beta$  participated in HG-induced HK-2 cell ferroptosis in a *Nrf-2*-dependent

manner, it may be interesting to know whether salusin- $\beta$  was changed in the process of ferroptosis. Western blotting results showed that the protein expression of salusin- $\beta$  was unexpectedly upregulated by several ferroptosis activators, including erastin ( $X_c^-$  inhibitors), *GPX4* inhibitors (RSL3 and FIN56) and GSH synthase inhibitor (buthionine sulfoximine) (Fig. 6A). Conversely, pretreatment of ferrostatin-1 (a ferroptosis inhibitor) downregulated the increased expression of salusin- $\beta$  in HG-treated HK-2 cells (Fig. 6B). These results suggested that interaction of salusin- $\beta$  with ferroptosis formed a positive feedback, thereby contributing to HG-induced HK-2 cell injury and DN.

## Discussion

The main findings in the current study were that salusin- $\beta$  expression was notably increased at protein and mRNA levels in HK-2 cells upon exposure to HG. *In vitro* results showed that deficiency of salusin- $\beta$  curbed, while overexpression of salusin- $\beta$  aggravated, lipoygenase activation, iron

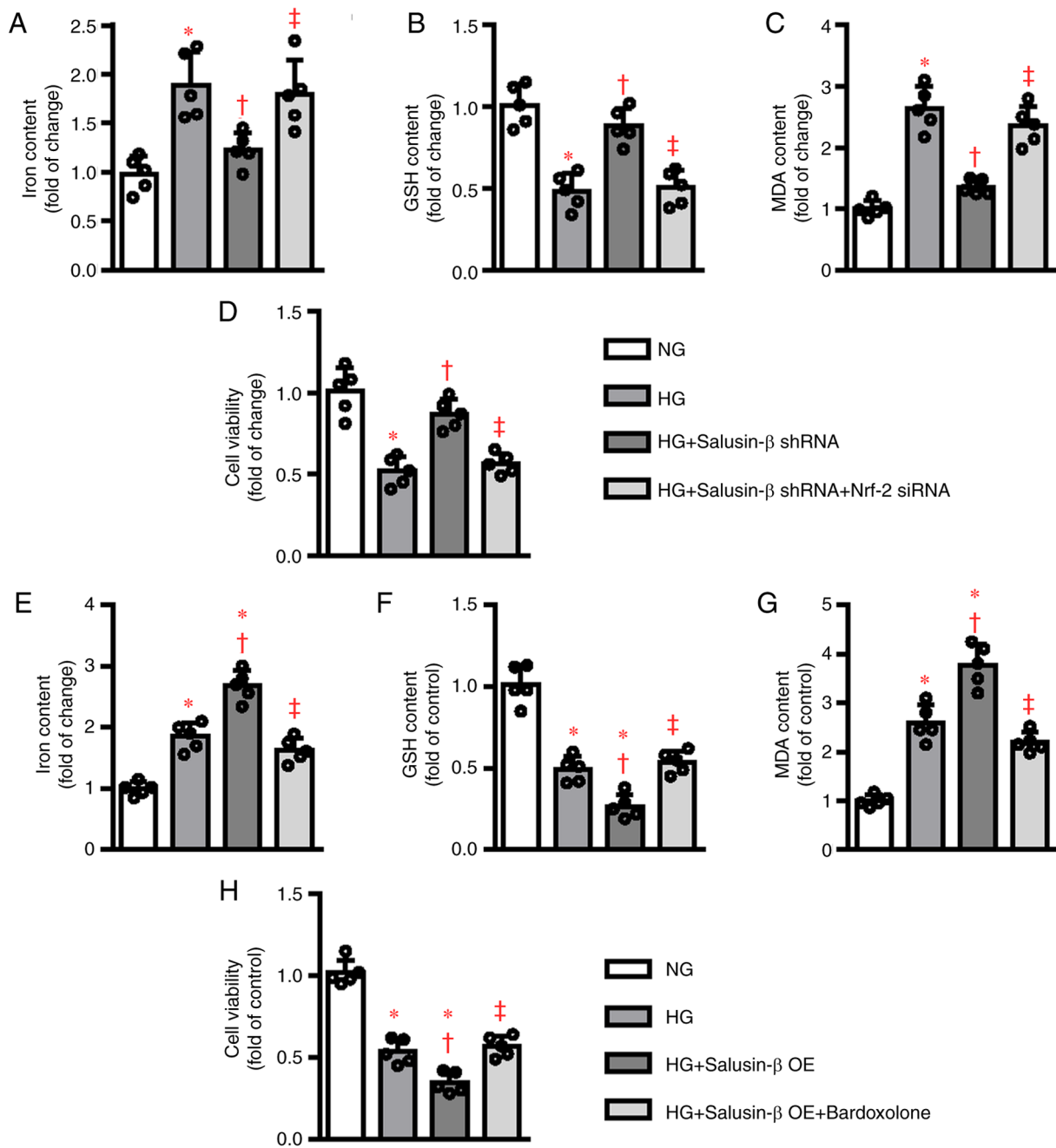


Figure 5. Modulation of *Nrf-2* signaling affected the roles of salusin-β in HG-induced ferroptosis. HK-2 cells were transduced with control siRNA and *Nrf-2* siRNA (50 nM) for 6 h and then transduced with lentivirus particles carrying salusin-β shRNA or negative control shRNA at MOI = 50 for 24 h and then challenged by HG stimulation for another 48 h. The (A) iron contents, (B) GSH contents, (C) MDA levels and (D) cell viability were then measured, respectively. HK-2 cells were pretreated with *Nrf-2* inducer bardoxolone methyl (100 nM) for 30 min and transduced with lentivirus expressing salusin-β vectors or empty vectors (MOI=50) for 48 h before administration of NG or HG for another 48 h. Afterwards, the (E) iron contents, (F) GSH contents, (G) MDA levels and (H) cell viability were then measured, respectively. Data are presented as the mean ± SD (n=5 per group). \*P<0.05 vs. NG. †P<0.05 vs. HG. ‡P<0.05 vs. HG + Salusin-β shRNA or HG + Salusin-β OE. *Nrf-2*, nuclear factor erythroid-derived 2-like 2; HG, high glucose; si, short interfering RNA; MOI, multiplicity of infection; NG, normal glucose; GSH, glutathione; MDA, malondialdehyde; sh, short hairpin RNA; OE, overexpression.

accumulation, GSH depletion, ROS accumulation in renal tubular epithelial cells induced by HG. Furthermore, it was found that salusin-β knockdown upregulated *Nrf-2* signaling to reduce HG-induced ferroptosis-related events, whereas salusin-β overexpression conferred the opposite effects. The importance of *Nrf-2* in salusin-β-mediated ferroptosis was further confirmed by the findings that knockdown of *Nrf-2* abolished the protective effects of salusin-β shRNA against HG-induced ferroptosis occurrence. By contrast, induction of

*Nrf-2* prevented the positive effects of salusin-β overexpression on ferroptosis progression induced by HG. Crucially, salusin-β protein expression was also increased by ferroptosis inducers, whereas ferroptosis inhibitor abrogated HG-induced salusin-β overexpression in HK-2 cells. Collectively, the results demonstrated for the first time, to the best of the authors' knowledge, that a salusin-β-ferroptosis signaling loop promoted the initiation and progression of renal tubular cell injury *in vitro*.

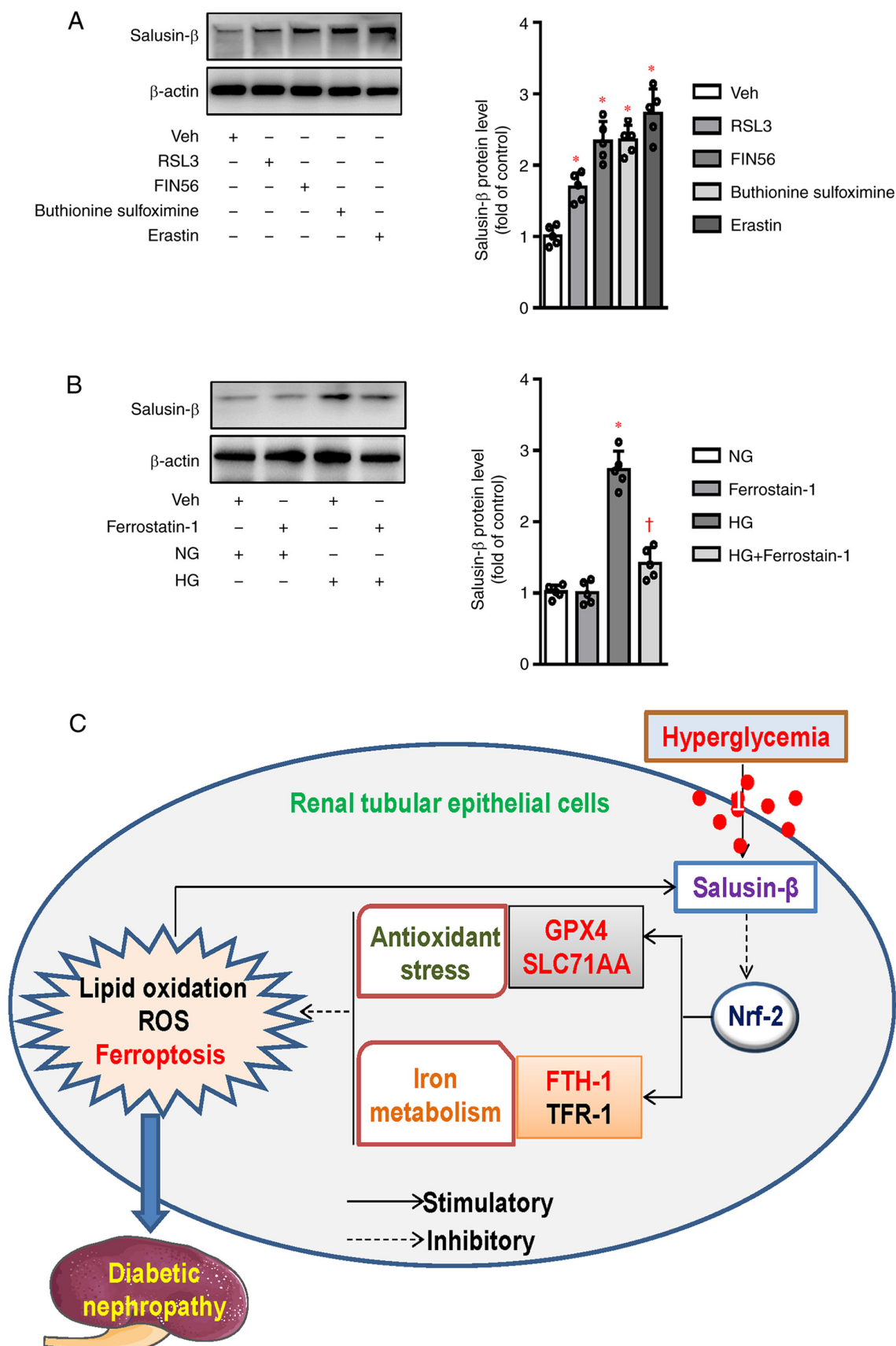


Figure 6. Expression of salusin- $\beta$  during the process of ferroptosis. (A) HK-2 cells were treated with ferroptosis activators for 24 h, including erastin (5  $\mu$ M), GPX4 inhibitors (1  $\mu$ M for RSL3 and 5  $\mu$ M for FIN56) and GSH synthase inhibitor (100  $\mu$ M for buthionine sulfoximine), the protein expression of salusin- $\beta$  was analyzed by western blotting. (B) HK-2 cells were pretreated with ferrostatin-1 (1  $\mu$ M) for 30 min and incubated with HG for 48 h, the protein expression of salusin- $\beta$  was then detected by western blotting. (C) The action mechanism of salusin- $\beta$  involved in ferroptosis in diabetic kidneys via inactivation of *Nrf-2* signaling. Data are presented as the mean  $\pm$  SD (n=5 per group). \*P<0.05 vs. Veh or NG. †P<0.05 vs. HG. GPX4, glutathione peroxidase 4; GSH, glutathione; *Nrf-2*, nuclear factor erythroid-derived 2-like 2; NG, normal glucose; HG, high glucose; Veh, Vehicle SLC7A11, solute carrier family 7 (cationic amino acid transporter, y+ system) member 11; FTH-1, ferritin heavy polypeptide 1; TFR-1, transferrin receptor 1; ROS, reactive oxygen species.



Iron, an essential mineral, is required for a variety of vital biological functions in health (52). The processes of iron metabolism are precisely regulated by numerous biological signals, including oxygen and lipid metabolism, protein production, cellular respiration and DNA synthesis (53). Iron-dependent cell death, generally known as ferroptosis, is a disorder of iron metabolism (54). Ferroptosis, a special type of regulated cell death that is different from necroptosis, apoptosis and other forms of cell death, is defined as iron overload, deposition of lipid peroxidation products, ROS overproduction and weakened antioxidant capacity (55). Studies have demonstrated that oxidative stress-induced ROS accumulation activates various signaling pathways, resulting in DNA damage and cell apoptosis (56,57). These studies indicate that oxidative stress is closely associated with both apoptosis and ferroptosis in cells. It has been indicated that ferroptosis is involved in the pathological mechanisms of numerous diseases, including diabetes, neurodegenerative diseases, atherosclerosis, obesity, non-alcoholic fatty liver disease and types of cancer (58). Notably, ferroptosis-related pathophysiological changes are also observed in DN (18,19). Fenofibrate, a ferroptosis inhibitor, reduces diabetes-induced ferroptosis in the kidneys and delays the progression of diabetic kidney disease (19). Salusin- $\beta$  is reported to be responsible for cisplatin-induced HK-2 cell injury via increasing MDA contents and ROS generation and decreasing GSH activity, implying the regulatory role of salusin- $\beta$  in acute kidney injury (35). The results present of the study, showed that HG stimulation dose- and time-dependently increased the protein and mRNA levels of salusin- $\beta$  in HK-2 cells, indicating that HG might be taken as a potential inducer for salusin- $\beta$  expression in HK-2 cells. Notably, knockdown of salusin- $\beta$  mitigated cell apoptosis, oxidative stress and iron deposition, but restored GSH contents in HG-incubated HK-2 cells. By contrast, overexpression of salusin- $\beta$  aggravated HG-induced cell apoptosis, ROS accumulation, antioxidant capacity reduction and iron deposition in HK-2 cells. These results clearly suggested that salusin- $\beta$  might serve as an important regulator in HG-triggered apoptosis and ferroptosis in HK-2 cells.

*GPX4* and *SLC7A11* are considered as important biomarkers of ferroptosis as deficiency of them might induce massive ROS production and GSH biogenesis dysfunction; key features for ferroptosis (59,60). *TFR-1* and *FTH-1*, two key genes involved in iron metabolism homeostasis, are closely linked with the development of ferroptosis (61,62). In line with previous results (19), the protein and mRNA expressions of *GPX4*, *SLC7A11* and *FTH-1* were downregulated, while *TFR-1* protein and mRNA expression levels were inhibited in HK-2 cells under HG treatment. All the above effects were reversed by silencing of salusin- $\beta$ , but were aggravated by overexpression of salusin- $\beta$ . When salusin- $\beta$  was absent, a homeostasis in *GPX4*, *SLC7A11*, *FTH-1* and *TFR-1* expressions decreased the sensitivity of HK-2 cells to ferroptosis induced HG. By contrast, overexpression of salusin- $\beta$  limited the ability of HK-2 cells to resist HG-induced ferroptosis through abnormal expressions of *GPX4*, *SLC7A11*, *FTH-1* and *TFR-1*. Overall, these observations suggested that salusin- $\beta$  contributed to HG-induced ferroptosis through regulation of genes for antioxidant system (*GPX4* and *SLC7A11*) and iron metabolism regulation system (*FTH-1* and *TFR-1*). Apart from these

ferroptosis markers, abnormal ultrastructural changes in the mitochondria are also observed in ferroptotic cells, including shrunken mitochondria, increased bilayer membrane density, mitochondrial ridge reduction or even disappearance and outer mitochondrial membrane disruption (8,10,63). Transmission electron microscopy is a well-known approach to reveal the presence of small mitochondria with increased mitochondrial membrane density and vanishing of mitochondrial cristae in ferroptotic cells (63). In the present study, the absence of mitochondrial transmission electron microscopy images is one of the limitations and thus transmission electron microscopy will be used to examine whether salusin- $\beta$  affects the alterations in mitochondrial morphology and cristae structure of HK-2 cells in the future. It is expected that mitochondrial transmission electron microscopy images would be required to further ascertain the role of salusin- $\beta$  in HG-induced HK-2 cell ferroptosis.

Studies reveal that *Nrf-2* is a dominant transcription factor that is responsible for cellular redox balance and *Nrf-2* degradation is observed in DN (19,64,65). Downregulation of *Nrf-2* is closely associated with diabetes-aggravated renal oxidative damage (66). Notably, *Nrf-2* signaling is implicated in the process of ferroptosis via regulating GSH homeostasis, lipid metabolism and mitochondrial functions (67). *Nrf-2* is documented to promote ferroptosis resistance via regulation of enzymes responsible for GSH synthesis (*SLC7A11*) and lipid peroxides neutralization (*GPX4*), as well as proteins fundamental for iron signaling (ferritin and ferroportin) (68,69). *Nrf-2* might afford a protection against ferroptosis-related diseases, including DN (19). Due to the importance of *Nrf-2* in anti-oxidative stress and iron metabolism, the present study investigated whether activation of *Nrf-2* signaling was associated with the protective effects of salusin- $\beta$  shRNA against HG-induced ferroptosis in HK-2 cells. In line with expectations, HG-induced downregulation of *Nrf-2* was largely rescued by silencing of salusin- $\beta$ , but was further decreased by overexpression of salusin- $\beta$ . Following *Nrf-2* silencing, the antagonistic effects of salusin- $\beta$  shRNA on ferroptosis disappeared. By contrast, induction of *Nrf-2* markedly limited the positive effects of salusin- $\beta$  overexpression on ferroptosis development in the context of diabetes. The data established that salusin- $\beta$  might be involved in the pathologies of DN-induced ferroptosis through negative regulation of the *Nrf-2* signaling.

The results also demonstrated that ferroptosis activators promoted the protein expression of salusin- $\beta$ , while inhibition of ferroptosis counteracted HG-induced expression of salusin- $\beta$  in HK-2 cells. However, the mechanisms that underlie ferroptosis- or HG-induced salusin- $\beta$  expressions in HK-2 cells remain to be elucidated, which merits further study. These preliminary results indicated that salusin- $\beta$  and ferroptosis form a positive feedback loop to contribute to HG-induced renal tubular cell injury. The second limitation of the present study was that the role of salusin- $\beta$  in HG-induced ferroptosis was only explored in cellular experiments. Thereafter, animal studies are required to further test the exact roles of salusin- $\beta$  in the pathologies of diabetes-induced renal ferroptosis and injury. These findings might provide novel insights into the molecular mechanisms underlying the roles of salusin- $\beta$  in diabetic kidney disease-related ferroptosis.

## Acknowledgements

Not applicable.

## Funding

No funding was received.

## Availability of data and materials

The datasets used and/or analyzed during the current study are available from the corresponding author on reasonable request.

## Authors' contributions

WW and XJ conducted the experiments and data analysis, preparation of figures, as well as manuscript preparation of manuscript. ZC and CG participated in interpretation of results and finalizing the manuscript for submission. ZC and CG were responsible for the drafting, revision and submission of this manuscript. WW and ZC confirm the authenticity of all the raw data. All authors read and approved the final manuscript.

## Ethics approval and consent to participate

Not applicable.

## Patient consent for publication

Not applicable.

## Competing interests

The authors declare that they have no competing interests.

## References

- Yang Y, Shi K, Patel DM, Liu F, Wu T and Chai Z: How to inhibit transforming growth factor beta safely in diabetic kidney disease. *Curr Opin Nephrol Hypertens* 30: 115-122, 2021.
- Feliers D, Lee HJ and Kasinath BS: Hydrogen sulfide in renal physiology and disease. *Antioxid Redox Signal* 25: 720-731, 2016.
- Alicic RZ, Cox EJ, Neumiller JJ and Tuttle KR: Incretin drugs in diabetic kidney disease: Biological mechanisms and clinical evidence. *Nat Rev Nephrol* 17: 227-244, 2021.
- Lin J, Cheng A, Cheng K, Deng Q, Zhang S, Lan Z, Wang W and Chen J: New insights into the mechanisms of pyroptosis and implications for diabetic kidney disease. *Int J Mol Sci* 21: 7057, 2020.
- Sun HJ, Wu ZY, Cao L, Zhu MY, Liu TT, Guo L, Lin Y, Nie XW and Bian JS: Hydrogen sulfide: Recent progression and perspectives for the treatment of diabetic nephropathy. *Molecules* 24: 2857, 2019.
- Dugbartey GJ: Diabetic nephropathy: A potential savior with 'rotten-egg' smell. *Pharmacol Rep* 69: 331-339, 2017.
- Sun HJ, Xiong SP, Cao X, Cao L, Zhu MY, Wu ZY and Bian JS: Polysulfide-mediated sulphydration of SIRT1 prevents diabetic nephropathy by suppressing phosphorylation and acetylation of p65 NF- $\kappa$ B and STAT3. *Redox Biol* 38: 101813, 2020.
- Dixon SJ, Lemberg KM, Lamprecht MR, Skouta R, Zaitsev EM, Gleason CE, Patel DN, Bauer AJ, Cantley AM, Yang WS, *et al*: Ferroptosis: An iron-dependent form of nonapoptotic cell death. *Cell* 149: 1060-1072, 2012.
- Wu D and Chen L: Ferroptosis: A novel cell death form will be a promising therapy target for diseases. *Acta Biochim Biophys Sin (Shanghai)* 47: 857-859, 2015.
- Tang D, Chen X, Kang R and Kroemer G: Ferroptosis: Molecular mechanisms and health implications. *Cell Res* 31: 107-125, 2021.
- Tang D and Kroemer G: Ferroptosis. *Curr Biol* 30: R1292-R1297, 2020.
- Latunde-Dada GO: Ferroptosis: Role of lipid peroxidation, iron and ferritinophagy. *Biochimica et biophysica acta. Biochim Biophys Acta Gen Subj* 1861: 1893-1900, 2017.
- Martin-Sanchez D, Ruiz-Andres O, Poveda J, Carrasco S, Cannata-Ortiz P, Sanchez-Niño MD, Ortega MR, Egido J, Linkermann A, Ortiz A and Sanz AB: Ferroptosis, but not necroptosis, is important in nephrotoxic folic acid-induced AKI. *J Am Soc Nephrol* 28: 218-229, 2017.
- Guerrero-Hue M, García-Caballero C, Palomino-Antolín A, Rubio-Navarro A, Vázquez-Carballo C, Herencia C, Martín-Sánchez D, Farré-Alins V, Egea J, Cannata P, *et al*: Curcumin reduces renal damage associated with rhabdomyolysis by decreasing ferroptosis-mediated cell death. *FASEB J* 33: 8961-8975, 2019.
- Lee H, Zandkarimi F, Zhang Y, Meena JK, Kim J, Zhuang L, Tyagi S, Ma L, Westbrook TF, Steinberg GR, *et al*: Energy-stress-mediated AMPK activation inhibits ferroptosis. *Nat Cell Biol* 22: 225-234, 2020.
- Li Z, Li J, Miao X, Cui W, Miao L and Cai L: A minireview: Role of AMP-activated protein kinase (AMPK) signaling in obesity-related kidney injury. *Life Sci* 15: 118828, 2020.
- Unsal V, Cicek M and Sabancilar I: Toxicity of carbon tetrachloride, free radicals and role of antioxidants. *Rev Environ Health* 24: doi: 10.1515, 2020.
- Wang Y, Bi R, Quan F, Cao Q, Lin Y, Yue C, Cui X, Yang H, Gao X and Zhang D: Ferroptosis involves in renal tubular cell death in diabetic nephropathy. *Eur J Pharmacol* 888: 173574, 2020.
- Li S, Zheng L, Zhang J, Liu X and Wu Z: Inhibition of ferroptosis by up-regulating Nrf2 delayed the progression of diabetic nephropathy. *Free Radic Biol Med* 162: 435-449, 2021.
- Shichiri M, Ishimaru S, Ota T, Nishikawa T, Isogai T and Hirata Y: Salusins: Newly identified bioactive peptides with hemodynamic and mitogenic activities. *Nat Med* 9: 1166-1172, 2003.
- Suzuki N, Shichiri M, Tateno T, Sato K and Hirata Y: Distinct systemic distribution of salusin- $\alpha$  and salusin- $\beta$  in the rat. *Peptides* 32: 805-810, 2011.
- Suzuki N, Shichiri M, Akashi T, Sato K, Sakurada M, Hirono Y, Yoshimoto T, Koyama T and Hirata Y: Systemic distribution of salusin expression in the rat. *Hypertension Res* 30: 1255-1262, 2007.
- Sato K, Watanabe R, Itoh F, Shichiri M and Watanabe T: Salusins: Potential use as a biomarker for atherosclerotic cardiovascular diseases. *Int J Hypertension* 2013: 965140, 2013.
- Watanabe T, Sato K, Itoh F, Iso Y, Nagashima M, Hirano T and Shichiri M: The roles of salusins in atherosclerosis and related cardiovascular diseases. *J Am Soc Hypertens* 5: 359-365, 2011.
- Kolakowska U, Olanski W and Wasilewska A: Salusins in hypertension and related cardiovascular diseases. *Curr Drug Metab* 17: 827-833, 2016.
- Wang WJ, Jiang X, Gao CC and Chen ZW: Salusin- $\alpha$  mitigates diabetic nephropathy via inhibition of the Akt/mTORC1/p70S6K signaling pathway in diabetic rats. *Drug Chem Toxicol* 31: 1-8, 2019.
- Fujimoto K, Hayashi A, Kamata Y, Ogawa A, Watanabe T, Ichikawa R, Iso Y, Koba S, Kobayashi Y, Koyama T and Shichiri M: Circulating levels of human salusin-beta, a potent hemodynamic and atherogenesis regulator. *PLoS One* 8: e76714, 2013.
- Kolakowska U, Kuroczycka-Saniutycz E, Wasilewska A and Olanski W: Is the serum level of salusin-beta associated with hypertension and atherosclerosis in the pediatric population? *Pediatr Nephrol* 30: 523-531, 2015.
- Yassien M, Fawzy O, Mahmoud E and Khidr EG: Serum salusin- $\beta$  in relation to atherosclerosis and ventricular dysfunction in patients with type 2 diabetes mellitus. *Diabetes Metab Syndr* 14: 2057-2062, 2020.
- Sipahi S, Genc AB, Acikgoz SB, Yildirim M, Aksoy YE, Vatan MB, Dheir H and Altundis M: Relationship of salusin-alpha and salusin-beta levels with atherosclerosis in patients undergoing haemodialysis. *Singapore Med J* 60: 210-215, 2019.
- Sahin I and Aydin S: Serum concentration and kidney expression of salusin- $\alpha$  and salusin- $\beta$  in rats with metabolic syndrome induced by fructose. *Biotech Histochem* 88: 153-160, 2013.
- Zhao MX, Zhou B, Ling L, Xiong XQ, Zhang F, Chen Q, Li YH, Kang YM and Zhu GQ: Salusin- $\beta$  contributes to oxidative stress and inflammation in diabetic cardiomyopathy. *Cell Death Dis* 8: e2690, 2017.

33. Sun H, Zhang F, Xu Y, Sun S, Wang H, Du Q, Gu C, Black SM, Han Y and Tang H: Salusin- $\beta$  promotes vascular calcification via nicotinamide adenine dinucleotide phosphate/reactive oxygen species-mediated klotho downregulation. *Antioxid Redox Signal* 31: 1352-1370, 2019.
34. Sun HJ, Chen D, Wang PY, Wan MY, Zhang CX, Zhang ZX, Lin W and Zhang F: Salusin- $\beta$  is involved in diabetes mellitus-induced endothelial dysfunction via degradation of peroxisome proliferator-activated receptor gamma. *Oxid Med Cell Longev* 2017: 6905217, 2017.
35. Lu QB, Du Q, Wang HP, Tang ZH, Wang YB and Sun HJ: Salusin- $\beta$  mediates tubular cell apoptosis in acute kidney injury: Involvement of the PKC/ROS signaling pathway. *Redox Biol* 30: 101411, 2020.
36. Zheng J and Conrad M: The metabolic underpinnings of ferroptosis. *Cell Metab* 32: 920-937, 2020.
37. Zhu X, Zhou Y, Cai W, Sun H and Qiu L: Salusin- $\beta$  mediates high glucose-induced endothelial injury via disruption of AMPK signaling pathway. *Biochem Biophys Res Commun* 491: 515-521, 2017.
38. Sun HJ, Liu TY, Zhang F, Xiong XQ, Wang JJ, Chen Q, Li YH, Kang YM, Zhou YB, Han Y, *et al*: Salusin- $\beta$  contributes to vascular remodeling associated with hypertension via promoting vascular smooth muscle cell proliferation and vascular fibrosis. *Biochim Biophys Acta* 1852: 1709-1718, 2015.
39. Szczesny-Malysiak E, Stojak M, Campagna R, Grosicki M, Jamrozik M, Kaczara P and Chlopicki S: Bardoxolone methyl displays detrimental effects on endothelial bioenergetics, suppresses endothelial ET-1 release and increases endothelial permeability in human microvascular endothelium. *Oxid Med Cell Long* 2020: 4678252, 2020.
40. Song X, Zhu S, Chen P, Hou W, Wen Q, Liu J, Xie Y, Liu J, Klionsky DJ, Kroemer G, *et al*: AMPK-mediated BECN1 phosphorylation promotes ferroptosis by directly blocking system  $X_c^-$  activity. *Curr Biol* 28: 2388-2399, 2018.
41. Zhu X, Wu S and Guo H: Active vitamin D and vitamin D receptor help prevent high glucose induced oxidative stress of renal tubular cells via AKT/UCP2 signaling pathway. *Biomed Res Int* 2019: 9013904, 2019.
42. Livak KJ and Schmittgen TD: Analysis of relative gene expression data using real-time quantitative PCR and the 2(-Delta Delta C(T)) method. *Methods* 25: 402-408, 2001.
43. Sun HJ, Zhang LL, Fan ZD, Chen D, Zhang L, Gao XY, Kang YM and Zhu GQ: Superoxide anions involved in sympathoexcitation and pressor effects of salusin- $\beta$  in paraventricular nucleus in hypertensive rats. *Acta physiol* 210: 534-545, 2014.
44. Sun HJ, Zhao MX, Ren XS, Liu TY, Chen Q, Li YH, Kang YM, Wang JJ and Zhu GQ: Salusin- $\beta$  promotes vascular smooth muscle cell migration and intimal hyperplasia after vascular injury via ROS/NF $\kappa$ B/MMP-9 pathway. *Antioxid Redox Signal* 24: 1045-1057, 2016.
45. Akpınar O, Özşimşek A, Güzel M and Nazıroğlu M: Clostridium botulinum neurotoxin A induces apoptosis and mitochondrial oxidative stress via activation of TRPM2 channel signaling pathway in neuroblastoma and glioblastoma tumor cells. *J Recept Signal Transduct Res* 40: 620-632, 2020.
46. Ma X, Zhang J, Wu Z and Wang X: Chicoric acid attenuates hyperglycemia-induced endothelial dysfunction through AMPK-dependent inhibition of oxidative/nitrative stresses. *J Receptor Signal Trans Res* 9: 1-15, 2020.
47. Lu QB, Sun JF, Yang QY, Cai WW, Xia MQ, Wu FF, Gu N and Zhang ZJ: Magnetic brain stimulation using iron oxide nanoparticle-mediated selective treatment of the left prefrontal cortex as a novel strategy to rapidly improve depressive-like symptoms in mice. *Zool Res* 41: 381-394, 2020.
48. Chen Q, Li Y, Luo J, Yang Y, Li J, Sun L, Xiao L, Xu X, Peng Y and Liu F: Effect of norcantharidin on the expression of FN, Col IV and TGF- $\beta$ 1 mRNA and protein in HK-2 cells induced by high glucose. *Zhong Nan Da Xue Xue Bao Yi Xue Ban* 37: 278-284, 2012 (In Chinese).
49. Lou JS, Zhao LP, Huang ZH, Chen XY, Xu JT, Tai WC, Tsim KW, Chen YT and Xi T: Ginkgetin derived from ginkgo biloba leaves enhances the therapeutic effect of cisplatin via ferroptosis-mediated disruption of the Nrf2/HO-1 axis in EGFR wild-type non-small-cell lung cancer. *Phytomedicine* 80: 153370, 2021.
50. Yu H, Guo P, Xie X, Wang Y and Chen G: Ferroptosis, a new form of cell death and its relationships with tumorous diseases. *J Cell Mol Med* 21: 648-657, 2017.
51. Song S, Gao Y, Sheng Y, Rui T and Luo C: Targeting NRF2 to suppress ferroptosis in brain injury. *Histol Histopathol* 36: 383-397, 2021.
52. Kobayashi M, Suhara T, Baba Y, Kawasaki NK, Higa JK and Matsui T: Pathological roles of iron in cardiovascular disease. *Curr Drug Targets* 19: 1068-1076, 2018.
53. Ravingerová T, Kindernay L, Barteková M, Ferko M, Adameová A, Zohdi V, Bernátová I, Ferenczyová K and Lazou A: The molecular mechanisms of iron metabolism and its role in cardiac dysfunction and cardioprotection. *Int J Mol Sci* 21: 7889, 2020.
54. Seibt TM, Proneth B and Conrad M: Role of GPX4 in ferroptosis and its pharmacological implication. *Free Radic Biol Med* 133: 144-152, 2019.
55. Wang Y, Peng X, Zhang M, Jia Y, Yu B and Tian J: Revisiting tumors and the cardiovascular system: Mechanistic intersections and divergences in ferroptosis. *Oxid Med Cell Longev* 2020: 9738143, 2020.
56. Yang L, Guan G, Lei L, Liu J, Cao L and Wang X: Oxidative and endoplasmic reticulum stresses are involved in palmitic acid-induced H9c2 cell apoptosis. *Biosci Rep* 39: BSR20190225, 2019.
57. Ma B, Guan G, Lv Q and Yang L: Curcumin ameliorates palmitic acid-induced saos-2 cell apoptosis via inhibiting oxidative stress and autophagy. *Evid Based Complement Alternat Med* 2021: 5563660, 2021.
58. Nechushtai R, Karmi O, Zuo K, Marjault HB, Darash-Yahana M, Sohn YS, King SD, Zandalinas SI, Carloni P and Mittler R: The balancing act of NEET proteins: Iron, ROS, calcium and metabolism. *Biochim Biophys Acta Mol Cell Res* 1867: 118805, 2020.
59. Chen X, Li J, Kang R, Klionsky DJ and Tang D: Ferroptosis: Machinery and regulation. *Autophagy* 26: 1-28, 2020.
60. Chen X, Yu C, Kang R and Tang D: Iron metabolism in ferroptosis. *Front Cell Dev Biol* 8: 590226, 2020.
61. Li LB, Chai R, Zhang S, Xu SF, Zhang YH, Li HL, Fan YG and Guo C: Iron exposure and the cellular mechanisms linked to neuron degeneration in adult mice. *Cells* 8: 198, 2019.
62. Fang X, Cai Z, Wang H, Han D, Cheng Q, Zhang P, Gao F, Yu Y, Song Z, Wu Q, *et al*: Loss of cardiac ferritin H facilitates cardiomyopathy via Slc7a11-mediated ferroptosis. *Circ Res* 127: 486-501, 2020.
63. Battaglia AM, Chirillo R, Aversa I, Sacco A, Costanzo F and Biamonte F: Ferroptosis and cancer: Mitochondria meet the 'Iron Maiden' cell death. *Cells* 9: 1505, 2020.
64. Mathur A, Pandey VK and Kakkar P: Activation of GSK3 $\beta$ /TrCP axis via PHLPP1 exacerbates Nrf2 degradation leading to impairment in cell survival pathway during diabetic nephropathy. *Free Radic Biol Med* 120: 414-424, 2018.
65. Wang S, Nie P, Lu X, Li C, Dong X, Yang F, Luo P and Li B: Nrf2 participates in the anti-apoptotic role of zinc in Type 2 diabetic nephropathy through wnt/ $\beta$ -catenin signaling pathway. *J Nutr Biochem* 84: 108451, 2020.
66. Rubin A, Salzberg AC, Imamura Y, Grivtishvilli A and Tombran-Tink J: Identification of novel targets of diabetic nephropathy and PEDF peptide treatment using RNA-seq. *BMC Genomics* 17: 936, 2016.
67. La Rosa P, Petrillo S, Turchi R, Berardinelli F, Schirinzi T, Vasco G, Lettieri-Barbato D, Fiorenza MT, Bertini ES, Aquilano K and Piemonte F: The Nrf2 induction prevents ferroptosis in friedreich's ataxia. *Redox Biol* 38: 101791, 2020.
68. Kerins MJ and Ooi A: The roles of NRF2 in modulating cellular iron homeostasis. *Antioxid Redox Signal* 29: 1756-1773, 2018.
69. Sun X, Ou Z, Chen R, Niu X, Chen D, Kang R and Tang D: Activation of the p62-Keap1-NRF2 pathway protects against ferroptosis in hepatocellular carcinoma cells. *Hepatology* 63: 173-184, 2016.



This work is licensed under a Creative Commons Attribution-NonCommercial-NoDerivatives 4.0 International (CC BY-NC-ND 4.0) License.